Design of a Compact and High-Efficiency 5.8 GHz Microwave Power Amplifier for Wireless Communication Systems

Luong Duy Manh[1(✉)], Nguyen Thanh Hung[1], Nguyen Thi Anh[1], Dai Xuan Loi[2], and Nguyen Huy Hoang[1]

[1] Le Quy Don Technical University,
236 Hoang Quoc Viet, Co Nhue 1, Hanoi, Vietnam
duymanhcs2@mta.edu.vn
[2] Military Institute of Science and Technology,
17 Hoang Sam, Cau Giay, Hanoi, Vietnam

Abstract. In this paper, a compact and low-cost, high-efficiency microwave power amplifier is proposed and designed. The proposed amplifier operates at the 5.8 GHz band for wireless communications systems. The amplifier is designed on a low-cost 5 W GaN HEMT transistor from Qorvo and a RO4350B substrate from Rogers. The high-efficiency can be obtained by treating the second harmonic at the input side. The output side is treated up to the third harmonic. Both small-signal and large-signal performance of the proposed amplifier were evaluated by both simulation and experiment. The simulated and measured results validate that the designed power amplifier can be realized in a compact size and delivered 5 W power with a high-efficiency at 5.8 GHz band.

Keywords: Power amplifier · GaN · HEMT · High-efficiency

1 Introduction

Power amplifiers (PA) play an essential role in radio systems. It is the element which consumes the most energy in the transmitter to ensure the required output power level of the system. Therefore, the PA must have high efficiency in order to save power supply as well as reduce the heat loss, increase operating duration and improve the stability of the PA performance. Recently, along with the method of improving linearity, improving efficiency is one of the main methods in the design of the PA. The typical method used to improve the efficiency of the PA includes using the class-E, class-F [1–4]. These two methods utilize short and open-circuit transmission lines to minimize the power loss at harmonics. In addition, the voltage and current waveform at the transistor are engineered to ensure they have no intersections in the time-domain, resulting in reduction

This research is funded by Vietnam National Foundation for Science and Technology Development (NAFOSTED) under grant number 102.04-2018.14.

N.-S. Vo et al. (Eds.): INISCOM 2021, LNICST 379, pp. 16–24, 2021.
https://doi.org/10.1007/978-3-030-77424-0_2

of the power loss at the transistor. The advantage of these two methods is that they ensure high efficiency because the power loss at the harmonics as well as the power loss at the transistor can be reduced simultaneously. However, these two methods have difficulties when PA works in the high-frequency range because the realization of the short- and open-circuited conditions at the high-frequency range is a challenging task.

Another typical efficiency improvement method is to make a phase adjustment between current and voltage at harmonics so that the phase difference between them is 90° [5–7], hence reducing the power consumption at the harmonics. The phase adjustment in the high-frequency range is easier to realize than creating short- and open-circuited condition. Therefore, this method is more suitable than using the class-E and class-F methods when designing PA operating in the high-frequency range.

Based on the above analysis, the research team has designed a high-efficiency PA operating at 5.8 GHz for use in the radio communication systems. Phase control method at the harmonics is used to improve the efficiency of the designed PA. The PA in this paper is designed using a low-cost GaN High-electron-mobility transistor (HEMT) device from Qorvo based on a microwave hybrid circuit technology.

The rest of the paper is structured as follows. In Sect. 2, the design procedure of the input and output matching networks of the PA is presented. In the Sect. 3, the simulated results will be experimentally verified at both small and large signal levels. Finally, Sect. 4 concludes the paper.

2 Impedance Matching Networks Design

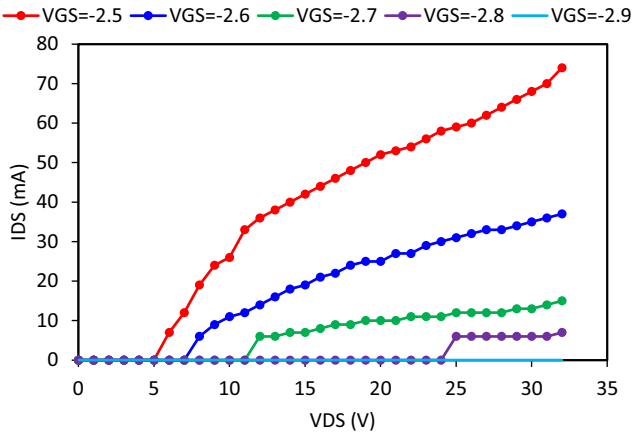

Fig. 1. Output characteristic of the real device.

In this paper, the simulation of the designed circuit is performed on Advanced Design System (ADS) [8] simulator from Keysight. The small-signal and

large-signal models of the transistor are provided by Qorvo [9]. The transistor used a GaN HEMT device. This device is packaged in a quad-flat no-leads (QFN) with a size of 3.0 cm × 3.0 cm. This device is low-cost and it has a wide operating frequency range from DC to 12 GHz with 5 W output power at 1 dB compression point. For the design process, we first determine the quiescent point or operation condition based on the transistor's characteristics. The bias condition as recommended by the manufacturer is: drain voltage $\mathbf{V_{ds}} = 32$ V and drain current $\mathbf{I_{ds}} = 25$ mA. Since the static characteristic of the model provided by Qorvo may differ from the actual transistor, the actual static characteristic of the actual transistor has to be measured. Figure 1 depicts the static output characteristic through actual measurement of the real transistor. Based on this characteristic, to set a bias drain current to 25 mA as recommended by the manufacturer, the gate voltage is set to $\mathbf{V_{gs}} = -2.73$ V. This is equivalent to the class-AB operation.

After setting up the operation condition, the impedance matching networks and bias circuit will be designed. These circuits are all made on the microstrip line technology using Rogers RO4350B material. The material parameters are as follows: dielectric constant: 3.66; dielectric loss: 0.0035; dielectric thickness: 30 mil; conductor thickness: 35 μm.

2.1 Input Matching Network

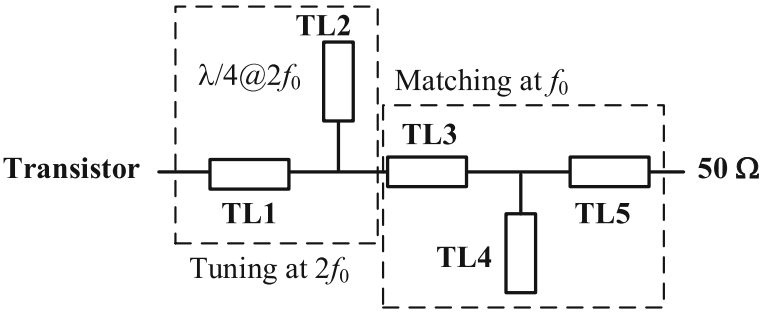

Fig. 2. Input matching network circuit.

The input circuit is responsible for transmitting the RF signal from the signal source to the input of the transistor so that the signal loss is minimal. This means that the input matching network (IMN) performs the impedance matching condition: $\mathbf{Z_S} = \mathbf{Z^*_{in}}$; where $\mathbf{Z_S}$ and $\mathbf{Z_{in}}$ are the source impedance and input impedance of the transistor, respectively. In this study, an additional stub to suppress quadratic harmonics at the input of the IMN is employed in order to further improve the efficiency of the designed PA. Circuit diagram of the IMN is shown in Fig. 2. Here, TL1, TL2 lines are used for the second harmonic

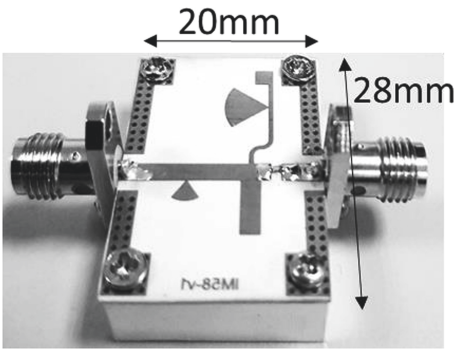

Fig. 3. Fabricated prototype of the IMN.

control while TL3, TL4 and TL5 lines are tuned to for impedance matching at the fundamental frequency. The fabricated prototype of the IMN is given in Fig. 3. The circuit shown in the figure includes the designed bias circuit. The circuit size is quite compact 2.0 cm × 2.8 cm. The optimum input impedance at the fundamental frequency and the second harmonic was determined using a Source Pull technique based on the large-signal model of the TGF2977-SM device provided by Qorvo. The results of the simulation of the electromagnetic (EM) level and the measured impedance results of the IMN are shown in Fig. 4. It can be seen the good agreement of the simulation results and the measurement of the impedance of the IMN, the impedance difference at the second harmonic is caused by the tolerance in the fabrication process of the microstrip lines. This causes the phase deviation between simulated and measured impedances. It is noted that the impedance at the second harmonic is located near the edge of the Smith chart, indicating that the phase difference between voltage and current at the second harmonic is approximately 90°, leading to a decrease in the power loss at the harmonic.

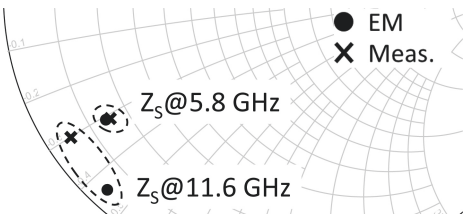

Fig. 4. Simulated and measured input impedances of the IMN.

In addition to the impedance, another important requirement of the matching network is the insertion loss which needs to be checked. Simulated and measured insertion losses of the IMN are shown in Fig. 5. It can be seen that the measurement of the insertion loss is greater than that of the simulation due to the loss

in the actual circuit taking into account the effect of the SMA connectors as well as the tolerance in the fabrication of microstrip lines. This difference will lead to a decrease in the output power as well as the power gain of the whole circuit.

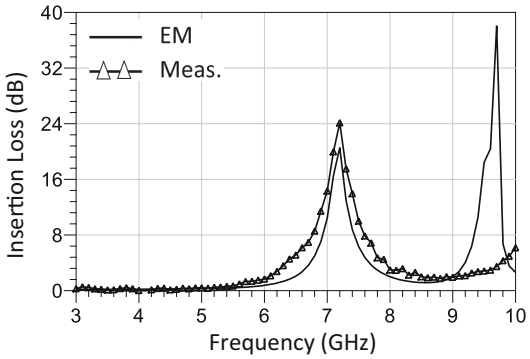

Fig. 5. Simulated and measured insertion loss of the IMN.

2.2 Output Matching Network

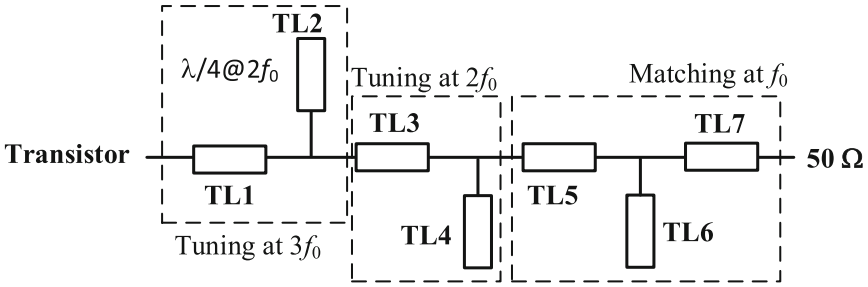

Fig. 6. OMN diagram.

The output matching network (OMN) plays a critical role in the design of the PA because it determines most of the important parameters of the PA such as output power, efficiency and power gain. Basically, the OMN is responsible for two main tasks: power matching to deliver the required output power to the load and compressing the high-order harmonics to improve the efficiency of the circuit. The OMN in this study, in addition to power matching task, will compress both the second and third harmonics. A Load Pull technique in ADS is used to determine the optimum impedances at the fundamental frequency and at the second harmonic and third harmonic. Schematic diagram of the OMN is shown in Fig. 6. Here, TL1, TL2 transmission lines adjust impedance for third harmonic

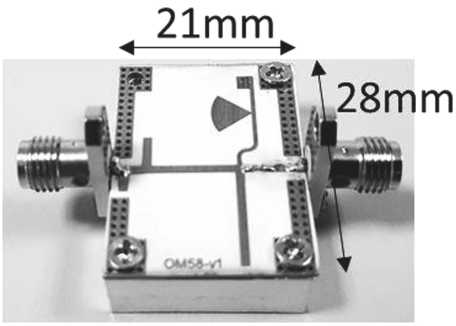

Fig. 7. Fabricated prototype of the OMN.

while TL3, TL4 adjust the second harmonic while TL5, TL6 and TL7 adjust the power matching at the fundamental frequency. The fabricated prototype of the OMN is shown in Fig. 7. It can be seen that the size of the OMN is also quite compact 2.1 cm × 2.8 cm. Simulated and measured impedances of the OMN are shown in Fig. 8. It is easy to see once again the good agreement between the simulation and measurement of the impedance of the OMN. This confirmed the accuracy of the design of the OMN. The impedances at the second and third harmonics of the OMN are also located near the edge of the Smith chart, implying that the power loss at these harmonics has been reduced, resulting in an enhanced efficiency. The losses in the OMN are shown in Fig. 9. The measurement results show that the insertion loss of the OMN is quite large compared to the simulation results, the same reason as with the IMN. This will lead to a decrease in the output power as well as the performance of the actual circuit compared to the simulation results.

3 Entire Circuit Evaluation

3.1 Small-Signal Evaluation

The results of simulation and measurement of the small signal parameters, or the scattering parameters, are shown in Fig. 10. It can be seen that the small signal measurement results is close to the simulation result at the electromagnetic field level. At the 5.8 GHz band, the input and output return losses are quite small, the small signal power gain is approximately 16 dB. Notably, the results of the small signal gain (S21) between the measurement and simulation are very close to each other. These results reflect the accuracy and suitability of designed circuits at the small signal level.

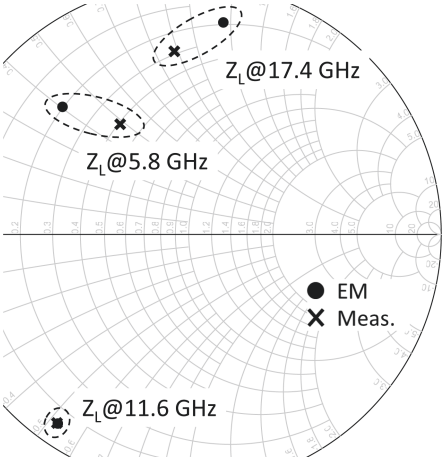

Fig. 8. Simulated and measured impedances of the OMN.

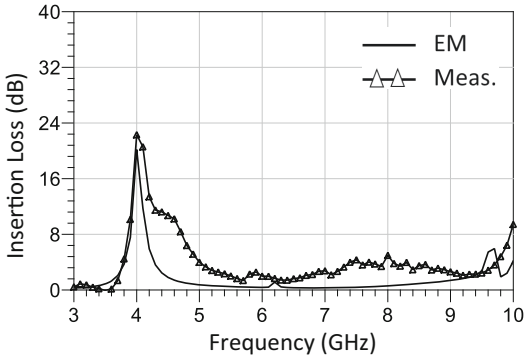

Fig. 9. Simulated and measured insertion loss of the OMN.

3.2 Large-Signal Evaluation

The results of the simulation and measurement of the large signal parameters are shown in Fig. 11. The evaluated criteria include: output power (Pout), efficiency (PAE) and power gain (Gain). It is noted that, the Qorvo's large signal model is used for the TGF2977-SM device, however the input/output matching networks use measured data as shown in the previous section. Another point is that the frequency used in the actual measurement is 5.72 GHz instead of 5.8 GHz as in the simulation. The frequency of 5.72 GHz is used because the actual measured insertion of the OMN is minimal. Observing the results in Fig. 11, it can be seen that, the output power and power gain between simulation and measurement have small differences. As indicated above, this difference is due to the difference in the insertion loss of the input and output matching circuits. However, the difference in PAE performance differs greatly in the large signal area. This

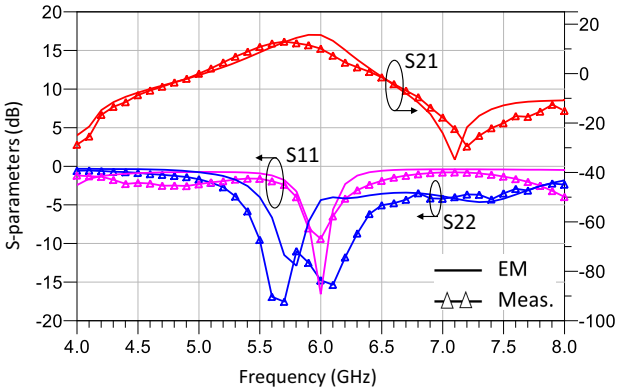

Fig. 10. Simulated and measured small-signal results.

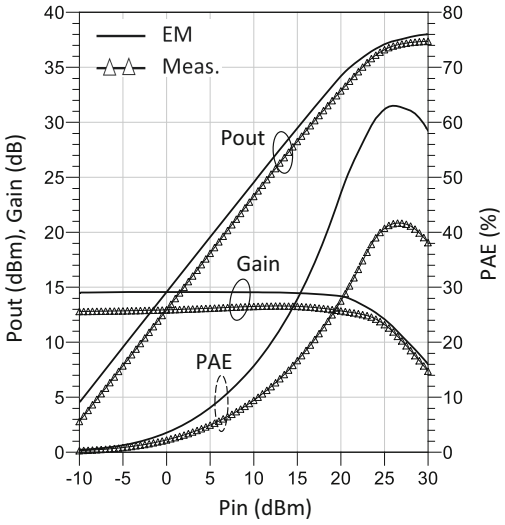

Fig. 11. Simulated and measured large-signal results.

difference is partly caused by the difference in output power. However, the bigger difference is due to the discrepancy between simulation and experiment in the drain current $\mathbf{I_{ds}}$. This deviation comes from the difference in the static characteristic between the simulation model and the actual device.

4 Conclusion

In this paper, we have presented the design method of a 5.8 GHz high-efficiency, microwave power amplifier. To improve efficiency, open-circuited stub are used to adjust the phase difference between the voltage and current at the second

harmonic at the input and the second and third harmonic at the output. The measurement results at the small signal level are close to the simulation results of the electromagnetic field level. Experimental results at the large signal level for the output power and power gain agree well with the simulation results. However, the PAE performance is quite different from the simulation because the DC model of the transistor is different from the actual model.

References

1. Sokal, N., et al.: Class EA new class of high-efficiency tuned single ended switching power amplifiers. IEEE J. Solid-State Circuits **SC-10**, 168–176 (1975)
2. Grebennikov, A.: High-efficiency class-e power amplifier with shunt capacitance and shunt filter. IEEE Trans. Circuits Syst. I Regul. Pap. **63**(1), 12–22 (2016)
3. Colantonio, P., et al.: On the class-F power amplifier design. Int. J. RF Microwave Comput.-Aided Eng. (1999)
4. Jin, X.X., et al.: High-efficiency filter-integrated class-F power amplifier based on dielectric resonator. IEEE Microwave Wirel. Compon. Lett. **27**(9), 827–829 (2017)
5. Kamiyama, M., et al.: 5.65 GHz high-efficiency GaN HEMT power amplifier with harmonics treatment up to fourth order. IEEE Microw. Wirel. Compon. Lett. **22**(6), 315–317 (2012)
6. Yao, T., et al.: Frequency characteristic of power efficiency for 10 W/30 W-class 2 GHz band GaN HEMT amplifiers with harmonic reactive terminations. In: Proceedings of the Asia-Pacific Microwave Conference, pp. 745–747 (2013)
7. Enomoto, J., et al.: Second harmonic treatment technique for bandwidth enhancement of GaN HEMT amplifier with harmonic reactive terminations. IEEE Trans. Microw. Theory Tech. **65**(12), 1–6 (2017)
8. https://www.keysight.com/zz/en/products/software/pathwave-design-software/pathwave-advanced-design-system.html
9. https://www.qorvo.com/